

Vortex shedding and surface pressures on a square cylinder at incidence to a uniform air stream

Jerry M. Chen ^{*}, Chia-Hung Liu

Department of Mechanical Engineering, National Chung Hsing University, Taichung 40227, Taiwan

Received 21 April 1998; accepted 16 April 1999

Abstract

This article describes results of experiments on vortex-shedding frequencies and surface pressures of a square cylinder at non-zero angle of incidence. The range of Reynolds numbers was 2000–21 000, but the lower range was emphasized. For Reynolds numbers greater than 5300, the Strouhal number shows a similar trend with changing angle of incidence; that is, a rapid rise in Strouhal number occurs at an angle of around 13°. The occurrence of such a jump in Strouhal number was found to be associated with onset of the flow reattachment, bringing in a strong pressure recovery on the lower side face of the cylinder. For lower Reynolds numbers $Re = 2000$ –3300, the maximum Strouhal number occurs at a relatively higher angle of 17°. Around this angle, the pressure measurements exhibit a rather weak pressure recovery, suggesting a less firm shear-layer reattachment to the side face of the cylinder. The nature of the reattaching flow was further examined by spectral analysis of the fluctuating pressure coefficients measured on the lower side face of the cylinder. © 1999 Elsevier Science Inc. All rights reserved.

Keywords: Square cylinder; Vortex shedding; Flow reattachment; Pressure recovery

1. Introduction

Rectangular cylinders are of a typical shape used for construction and equipment. Flows past structures with such a cross-sectional shape are susceptible to flow-induced vibration caused by vortex shedding and/or galloping instability. On the other hand, the unsteady character of the shedding process may provide a means to enhance heat transfer, particularly for equipment components exposed to a laminar flow environment (Igarashi, 1985, 1986). The phenomenon of vortex shedding from a rectangular cylinder depends largely upon the approaching flow characteristics and the angle of incidence to the flow. Although the shedding behavior may also be complicated by a change in the length-to-width ratio of the cylinder (Nakaguchi et al., 1968; Bearman and Trueman, 1972), the square section is the most frequently employed shape for investigations of this unsteady flow.

One of the principal features of vortex shedding from a bluff body is illustrated in terms of Strouhal number. For a square cylinder at an angle of incidence ($0 \leq \alpha \leq 45^\circ$) to the flow, the Strouhal numbers and/or drag coefficients were measured by a number of authors (e.g. Lee, 1975; Obasaju, 1983; Igarashi, 1984; Knisely, 1990; Norberg, 1993). These results led to an indication that the minimum drag coefficient occurs when the cylinder rotates to an angle near 13° where the Strouhal number rises sharply to reach a maximum.

Rockwell (1977) and Obasaju (1983) related the occurrence of maximum Strouhal number to reattachment of the separated shear layer. It is thought that the shear layer deflects at the reattachment point near the downstream corner of the cylinder and then rolls up at a distance downstream of the body to form a thin wake containing weaker vortices, causing a higher base pressure and hence smaller drag. At the same time, the thin wake suggests a contraction of the distance between the shed vortices in both transverse and longitudinal directions. This also results in a higher shedding frequency. It should be noted that the exact angle where reattachment begins to occur depends on the turbulence level and the Reynolds number as well (Vickery, 1966; Lee, 1975). Furthermore, the surface pressures that substantiated the onset of shear-layer reattachment provided by the aforementioned studies were measured at rather high Reynolds numbers ($7.5 \times 10^3 \leq Re \leq 2.5 \times 10^5$), and the Reynolds number over this high range appears to have no substantial influence on the measurements. However, in contrast to the high Reynolds number range, according to the Strouhal number measurements of Okajima (1982), a square cylinder may have a significant Reynolds number dependence for approximately $Re \leq 5 \times 10^3$. Understanding of flow characteristics around a square cylinder in such a low Reynolds number range ($Re \leq 5 \times 10^3$) has practical applications related to electronics cooling that has received increasing attention in design and manufacture of electronic equipment. Nevertheless, detailed information involving the vortex-shedding characteristics and the associated pressure distribution in the low Reynolds number range has remained limited.

^{*} Corresponding author.

E-mail address: jerry@dragon.nchu.edu.tw (J.M. Chen)

This article presents an experimental investigation of turbulent flow around a square cylinder at non-zero angle of incidence. The range of Reynolds numbers was between 2.0×10^3 and 2.1×10^4 , but the lower range was emphasized. Measurements of Strouhal numbers and surface pressure coefficients were carried out to reveal the combined influence of Reynolds number and angle of incidence on the patterns of separated shear layer and vortex formation. The variation of vortex-shedding characteristics with Reynolds number is discussed in detail, particularly for the range of angles corresponding to reattachment of the flow to the cylinder.

2. Experimental arrangement

The experiments were performed in a low-speed open-type wind tunnel with a square test section of $305 \text{ mm} \times 305 \text{ mm}$ and a length of 1100 mm. The flow into the test section had turbulence levels less than 0.5% for the velocity range tested in the experiments. Fig. 1 illustrates the flow configuration of the present study. The cylinder of $20 \text{ mm} \times 20 \text{ mm}$ square cross-section was centered on the mid-height of the test section, and spanned the width of the test section. The cylinder model was made from plexiglass, and was machined sharp edges. The angle of incidence α relative to the uniform freestream was varied in the range of $0 \leq \alpha \leq 45^\circ$ to an accuracy of within $\pm 0.5^\circ$.

Vortex shedding from the square cylinder was detected using a constant-temperature anemometer (TSI IFA 100) in conjunction with a hot-wire probe. The shedding frequency was measured on a spectrum analyzer (HP 3582) which was able to display the response in both time and frequency domains. During each measurement of vortex-shedding frequency, the probe was placed in the centerplane of the test section at a downstream station of $3\text{--}5D$ behind the test cylinder, where D is the width of the cylinder. The transverse position of the probe was set at a distance of about $2D$ above the centerline of the wake to preclude interference in the velocity signal from vortices of opposite sign. The mean spectra were averaged over at least twenty individual spectra yielding an uncertainty of $\pm 0.1 \text{ Hz}$ in the vortex-shedding frequency. All Strouhal numbers (St) presented are based on the most dominant shedding frequency, the projected cross-stream cylinder dimension, and the freestream velocity.

For measurements of surface pressures on the cylinder, nine pressure tappings of 0.75 mm in diameter were instrumented on its four sides at the mid-span. These pressure tappings were distributed at unequal spacing on each side. The cylinder was rotated by 90° at a time, so that rather fine pressure distributions could be measured on four sides of the cylinder. The pressures were measured using Setra 239 differential pressure transducers with a pressure range of 6.35 mm water. The transducers were connected to the pressure tappings with short

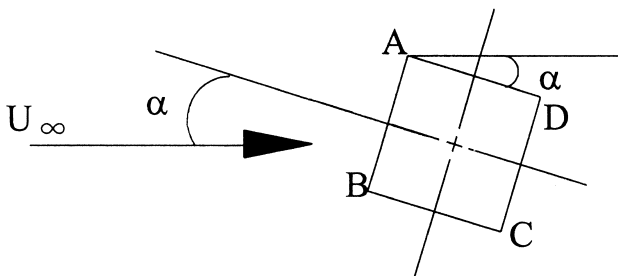


Fig. 1. Flow configuration and symbol definition.

Tygon tubes of equal length and in reference to the freestream wall pressure. The frequency response of the pressure transducer was higher than 2.0 kHz. Although the connection of the tubing to the transducer could reduce the overall dynamic response, such an arrangement for measurements sufficed for the dynamic range of interest in the present study. The pressure signals were recorded by a multi-channel analog data acquisition memory (ADAM ADC0512) which had an individual A/D converter on each channel. Each of the mean pressures was obtained via integrating the time history data for over 40–80 s, dependent on the freestream velocity. The estimated uncertainty (due to random errors) in the mean pressure coefficient C_p was approximately within ± 0.01 . The measurements of surface pressures and shedding frequencies were performed for freestream velocity U_∞ in the range 1.5–16.0 m/s, corresponding to Reynolds number $Re = U_\infty D/\nu$ in the range 2000–21 000, where ν is the kinematic viscosity.

In addition, a spanwise row of ten pressure tappings was placed along the centerline of the base of the cylinder to check for the extent of three-dimensionality of the flow. The mean base pressures measured across the span of the cylinder were found to be uniform (having a deviation of within $\pm 1\%$) over the center 40% of the span at $Re = 2000\text{--}2700$. At higher Reynolds numbers ($Re \geq 5300$), the spanwise uniformity of the base pressure extended to more than 60% of the span. Accordingly, three-dimensionality may not significantly affect the measurements presented (Armstrong and Barnes, 1986). Details involving the spanwise pressure measurements can be found in a conference paper of Chen and Liu (1997). Moreover, none of the results presented were corrected for the effects of wind-tunnel blockage. The geometric blockage due to the cylinder model was in the range between 6.6 and 9.3%.

3. Results and discussion

Measurements of surface pressure were made for the cylinder at zero incidence prior to examining the effects due to the change in the angle of incidence. Fig. 2 depicts the circumferential distribution of mean pressure coefficients around the zero-incidence cylinder for $Re = 2000\text{--}16000$. In this Figure,

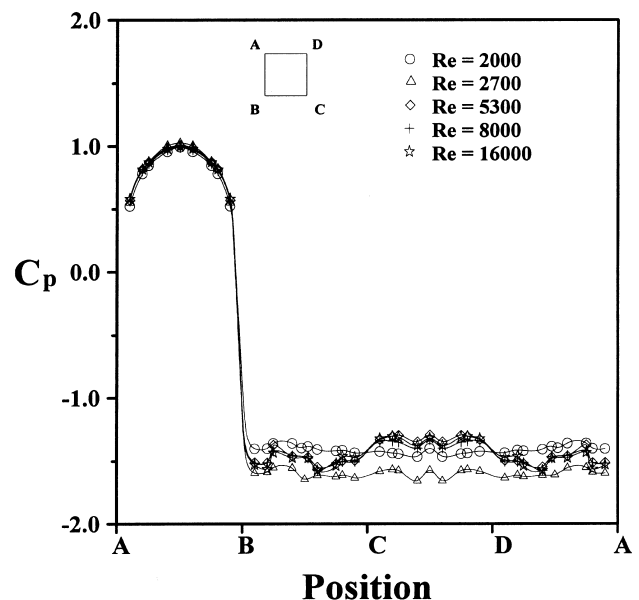


Fig. 2. Mean pressure coefficient distributions around the cylinder at $\alpha = 0^\circ$ for $Re = 2000\text{--}16000$.

AB is the windward face normal to the flow, BC and DA are the side faces parallel to the flow, and CD is the rear face. It can be seen that the Reynolds number has no discernible effect on the pressure coefficient distribution on the front face AB. However, the pressure distributions on the side and rear faces BCDA appear to differ for the lower Reynolds numbers $Re = 2000$ – 5300 , while they fall into nearly the same curve for $Re \geq 5300$. The difference in pressure distributions on BCDA for the lower Reynolds number range is associated with the variation of the distance required for vortex formation behind the body and the strength of the formed vortices (Bearman and Trueman, 1972; Roshko, 1993). At $Re = 2000$, a rather flat distribution of pressures at around $C_p = -1.35$ on BCDA may be attributed to the fact that the shear layers originating at the leading edges of the cylinder roll up at a relatively larger distance behind the cylinder to form a thick wake. As the Reynolds number is increased to $Re = 2700$, the pressure coefficients on BCDA substantially decrease to between -1.55 and -1.65 , indicating a shorter vortex formation length and a thinner wake width as well. At higher Reynolds numbers $Re = 5300$ – 16000 , the pressure tapers off towards the center of the rear face with a base pressure coefficient level exceeding the level found at $Re = 2000$. The rise of the base pressure for Reynolds numbers in the higher range is possibly caused by vortices of weak structures formed behind the cylinder.

When the cylinder is set at non-zero angle of incidence to the freestream, the mean flow structure is no longer symmetric about the centerline of the body. The formation of the vortices behind the cylinder may in turn change with the rotation angle. Fig. 3 shows the Strouhal numbers as a function of the angle of incidence for Reynolds numbers between 2000 and 21000. These Strouhal numbers are directly correlated to the angle of incidence. At relatively small angles of incidence, the Strouhal number value rises rapidly. It then levels out between $St = 0.17$ and 0.18 with a further increase in angle of incidence. Fig. 4 presents a plot of α_{\max} against Reynolds number, where α_{\max} denotes the angle where the Strouhal number increases to a maximum. The sudden jump occurs at $\alpha = 17^\circ$ for $Re = 2000$ – 3300 , and then decreases gradually as the Reynolds number increases from 3300 to 8000. At higher Reynolds numbers, α_{\max} remains steady at 13° . A number of authors also reported this

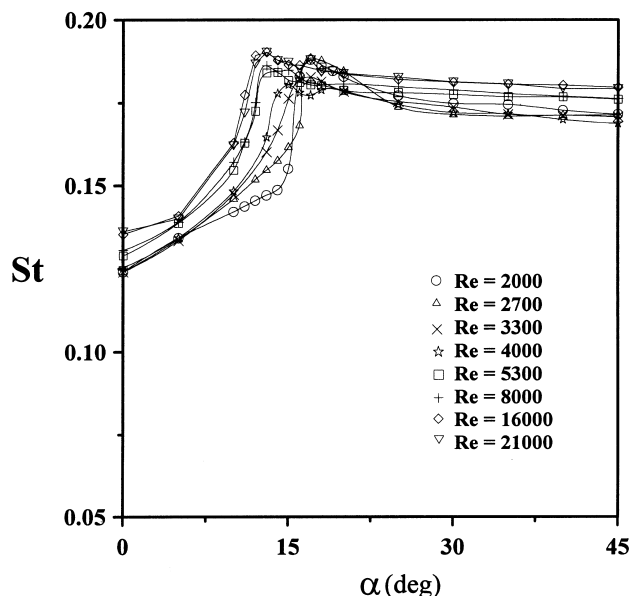


Fig. 3. Strouhal number as a function of the angle of incidence for $Re = 2000$ – 21000 .

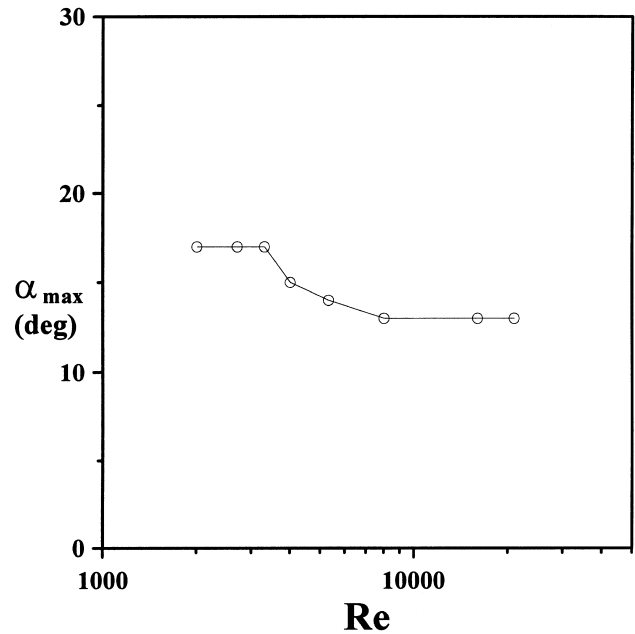


Fig. 4. Variation of the angle of the maximum Strouhal number with the Reynolds number.

sudden jump at around $\alpha = 13^\circ$ for Reynolds numbers in the higher range ($Re \geq 8000$). The jump in Strouhal number has been associated with the reattachment of the separated shear layer (Rockwell, 1977; Obasaju, 1983; Knisely, 1990). Nevertheless, for lower Reynolds numbers $Re \leq 5300$, Fig. 3 exhibits significant influence of the Reynolds number on the variation of the Strouhal number with the angle of incidence, particularly for angles nearing α_{\max} . In this lower Reynolds number range, the flow features around the cylinder may alter with the change in Reynolds number at angles near α_{\max} . This occurrence at the lower Reynolds numbers deserves further investigation.

Fig. 5 presents the circumferential distributions of pressure coefficients measured at different angles of incidence for $Re = 2700$ and 5300 . The pressure distribution on the front face varies with the rotation of the cylinder: as α increases, the position of maximum pressure shifts from the centerline to the lower corner. Again, the Reynolds number has no influence on the front face pressures. At $Re = 2700$, the C_p level on the rear and upper side faces CDA increases gradually with increasing α until the sudden jump angle $\alpha = 17^\circ$, and then at $\alpha = 25^\circ$ the level is lowered again. Accordingly, the cylinder has a minimum drag coefficient C_D at the sudden jump angle. On the lower side face BC, a pressure recovery begins to appear at the jump angle $\alpha = 17^\circ$, signifying possible reattachment of the shear layer. It is found that C_p values in the forward half portion drop below those measured at $\alpha = 10^\circ$ and 13° but still exceed those at zero incidence. The recovered pressure coefficient ΔC_p , which is defined as the difference between the maximum and minimum pressure coefficients measured on the side face, is about 0.55. The recovered pressure remains unchanged at $\alpha = 20^\circ$. As the angle of incidence is further increased to $\alpha = 25^\circ$, Fig. 5a demonstrates that the pressure coefficients on the side face BC rise markedly to reach a maximum of $C_p = -0.26$. This pressure rise may be a consequence of the attachment of the shear-layer flow to the side face.

For the case of $Re = 5300$, the angle of sudden jump in Strouhal number occurs at $\alpha = 14^\circ$, a smaller angle than that

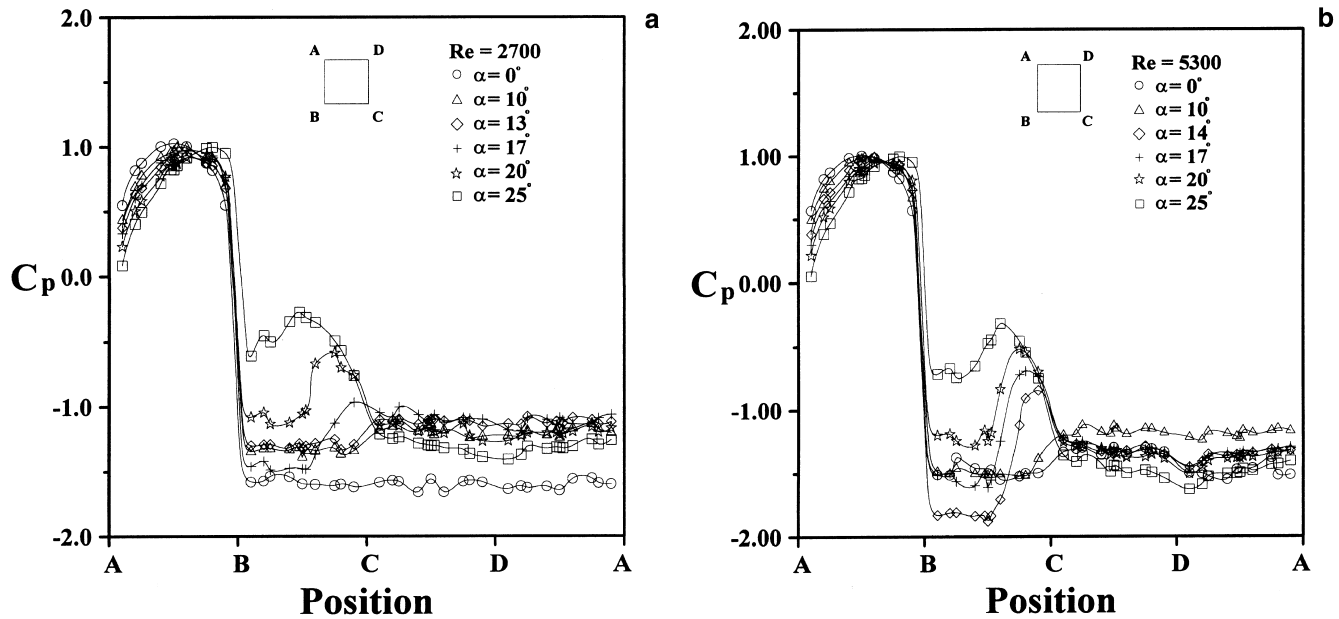


Fig. 5. Mean pressure coefficient distributions around the cylinder at various angles of incidence for: (a) $Re = 2700$; (b) $Re = 5300$.

for the case of $Re = 2700$. Fig. 5b displays that the side face (BC) pressure distribution is characterized by a plateau of low pressure followed by a recovery to a higher pressure nearing the trailing edge. The recovered pressure coefficient ΔC_p on the side face is about 1.05. The low pressure plateau as well as the strong pressure recovery indicates reattachment of the separated shear layer to the lower side face and a more constructed separation bubble than the bubble which occurs for $Re = 2700$. The reattachment of the shear layer was confirmed by our smoke-wire visualization (not shown). As the angle is increased to $\alpha = 17^\circ$ and 20° , the strong pressure recovery persists, despite the move-up of the pressure plateau. When the cylinder is rotated to $\alpha = 25^\circ$, the coefficient C_p on the lower side face BC rises to -0.31 . Thereafter, the pressure on the rear face CD drops sharply to a level below that measured at zero incidence. This phenomenon implies the existence of an attached shear-layer to the lower side face and the formation of a rather compact and close vortex just behind the rear face.

In order to further understand the nature of shear-layer reattachment and vortex shedding, pressure spectral measurements were attempted at two locations of the lower side face BC, one near the leading edge ($0.2D$ from edge B) and the other near the trailing edge ($0.8D$ from edge B). The pressure spectra measured near the leading edge are dominated by the vortex shedding and their significance is in line with the Strouhal frequency variation of Fig. 3. Herein, only the spectra of pressure fluctuation corresponding to pressures measured near the trailing edge are presented. Fig. 6 shows the comparison of the spectra acquired at angles near α_{\max} with those obtained for a fully separated flow at $\alpha = 10^\circ$ and for the attached shear-layer flow at $\alpha = 25^\circ$. It is quite clear that at a smaller angle $\alpha = 10^\circ$, the most pronounced peak frequency is due to the contribution of vortex shedding. As the angle approaches α_{\max} , the peak amplitude contributed by vortex shedding is largely depressed (see $\alpha = 16^\circ$ and $\alpha = 13^\circ$ for $Re = 2700$ and 5300 , respectively). At the angle of maximum Strouhal number, $\alpha = 17^\circ$ and $\alpha = 14^\circ$ for $Re = 2700$ and 5300 , respectively, the contribution due to vortex shedding drops to a minimum. For $Re = 5300$, amplitudes of low frequencies of about $1/30$ – $1/10$ the vortex-shedding frequency become appreciable at $\alpha = 14^\circ$. The appearance of low frequency pressure

fluctuation may be attributable to the instability of the onset of the shear-layer reattachment (Rockwell, 1977; Kiya and Sasaki, 1983; Cherry et al., 1984). However, the low frequency pressure fluctuation is not observed for $Re = 2700$, possibly because of the weak reattachment of the flow which occurs at a relatively higher onset angle for this case. At an angle slightly larger than α_{\max} , the contribution due to vortex shedding becomes visible. In the case of $Re = 2700$, this contribution is seen at $\alpha = 18^\circ$, whereas the contribution is less apparent in the case of $Re = 5300$ at $\alpha = 15^\circ$. For the attached flow taking place at $\alpha = 25^\circ$, the vortex shedding contribution again dominates the spectrum.

4. Conclusions

Experiments have been performed to investigate the flow around a square cylinder at non-zero angles of incidence to a uniform air stream. The vortex shedding frequencies and surface pressures were measured for Reynolds numbers between 2000 and 21 000, but the lower range ($Re \leq 5300$) was emphasized. As the cylinder is rotated with increasing angle of incidence, the Strouhal number rises sharply to reach a maximum at relatively small angles. Moreover, the Reynolds number in the lower range appears to have significant influence on the variation of the Strouhal number with the angle of incidence. An increase in Reynolds number in the lower range tends to promote the occurrence of the maximum Strouhal number from $\alpha = 17^\circ$ to 14° . The pressures measured at $Re = 5300$ for the cylinder at the angle where the maximum Strouhal number occurs exhibit a strong pressure recovery on the lower side face, indicating the onset of reattachment of the shear layer to the side face. The strong pressure recovery persists until the angle of incidence reaches $\alpha = 25^\circ$, where the wedge flow of attached shear layer to the side face may begin to develop. In contrast to the observation at $Re = 5300$, the measurements carried out at the lower Reynolds number $Re = 2700$ display a rather small recovered pressure coefficient at the angle corresponding to the rapid rise in Strouhal number. A less firm reattachment of the shear layer to the side face may account for such a weak pressure recovery. The pressure

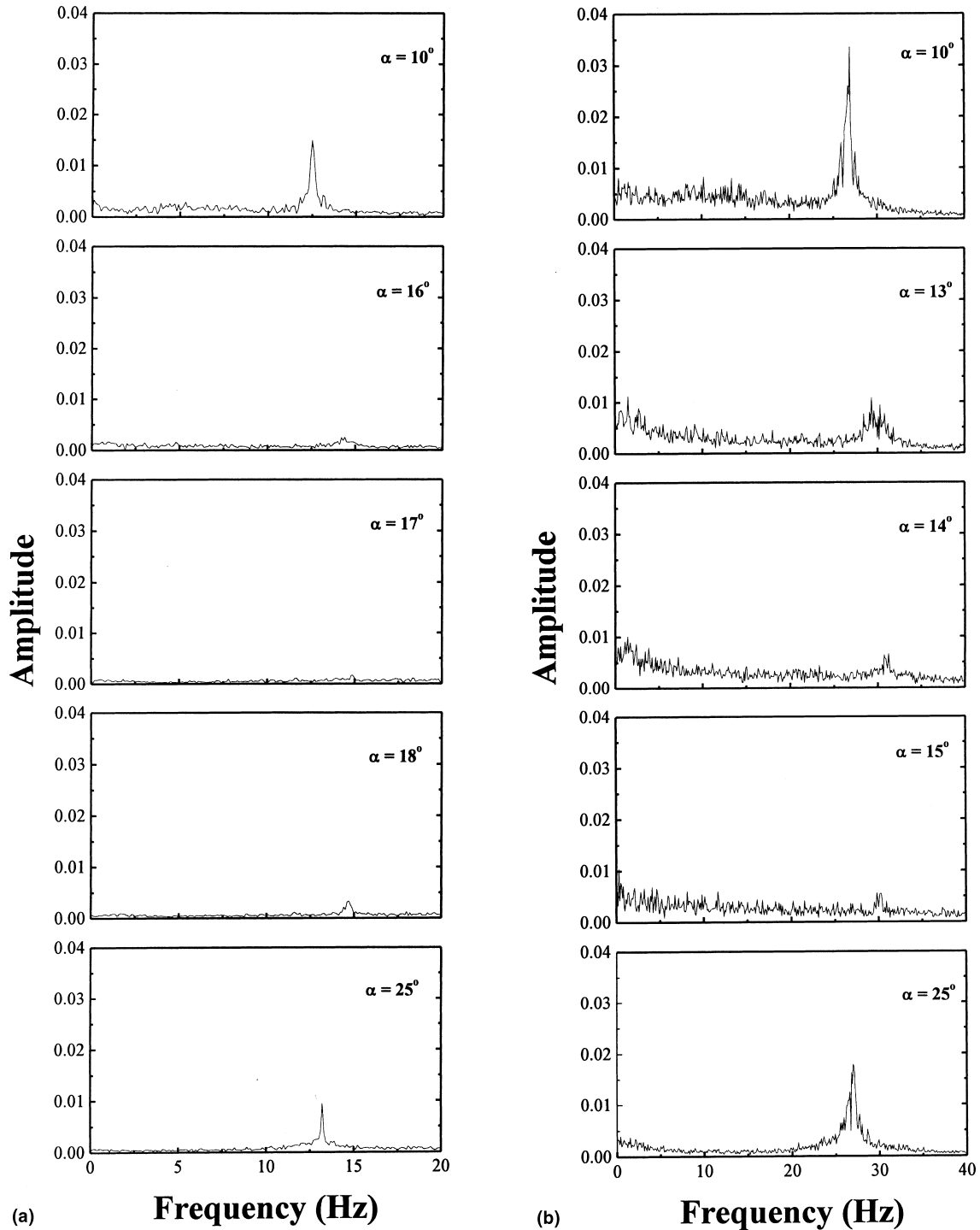


Fig. 6. Spectra of pressure fluctuation coefficient measured near the trailing of the cylinder at different angles of incidence for: (a) $Re = 2700$; (b) $Re = 5300$.

spectra measured at the lower side face of the cylinder show that the fluctuation amplitude contributed by the vortex shedding frequency drops to a minimum as the cylinder is rotated to the angle corresponding to the maximum Strouhal frequency. The pressure fluctuations of low frequencies at about $1/30$ – $1/10$ the Strouhal frequency can be observed in the spectra for $Re = 5300$ but not for $Re = 2700$. These fluctuations may be enhanced during the onset of flow reattachment to the side face. This is again a consequence of the weak reattach-

ment of the shear layer that occurs for the lower Reynolds number $Re = 2700$ at the angle of incidence corresponding to the maximum Strouhal frequency.

References

- Armstrong, B.J., Barnes, F.H., 1986. The effects of a perturbation on the flow over a bluff body. *Phys. Fluids* 29, 2095–2102.

- Bearman, P.W., Trueman, D.M., 1972. An investigation of the flow around rectangular cylinders. *Aeronaut. Q* 23, 229–237.
- Chen, J.M., Liu, C.-H., 1997. Vortex shedding and pressure distributions of a square cylinder in uniform stream. In: *Proceedings of the 21st National Conference on Theoretical and Applied Mechanics*, Taichung, Taiwan, 1 pp. 187–194.
- Cherry, N.J., Hillier, R., Latour, M.E.M.P., 1984. Unsteady measurements in a separated and reattaching flow. *J. Fluid Mech.* 144, 13–46.
- Igarashi, T., 1984. Characteristics of the flow around square prisms. *Bull. JSME* 27, 1858–1865.
- Igarashi, T., 1985. Heat transfer from a square prism to an air stream. *Internat. J. Heat Mass Transfer* 28, 175–181.
- Igarashi, T., 1986. Local heat transfer from a square prism to an air stream. *Internat. J. Heat Mass Transfer* 29, 777–784.
- Kiya, M., Sasaki, K., 1983. Structure of a turbulent separation bubble. *J. Fluid Mech.* 137, 83–113.
- Knisely, C.W., 1990. Strouhal numbers of rectangular cylinders at incidence: A review and new data. *J. Fluids Structures* 4, 371–393.
- Lee, B.E., 1975. The effect of turbulence on the surface pressure field of a square prism. *J. Fluid Mech.* 69 (2), 263–282.
- Nakaguchi, H., Hashimoto, K., Muto, S., 1968. An experimental study of aerodynamic drag of rectangular cylinders. *J. Japan Soc. Aeronaut. Space Sci.* 16, 1–5.
- Norberg, C., 1993. Flow around rectangular cylinders: pressure forces and wake frequencies. *J. Wind Eng. Indust. Aerodyn.* 49, 187–196.
- Obasaju, E.D., 1983. An investigation of the effects of incidence on the flow around a square section cylinder. *Aeronaut. Q.* 34, 243–259.
- Okajima, A., 1982. Strouhal numbers of rectangular cylinders. *J. Fluid Mech.* 123, 379–398.
- Rockwell, D.O., 1977. Organized fluctuations due to flow past a square cross section cylinder. *J. Fluids Engrg.* 99, 511–516.
- Roshko, A., 1993. Perspectives on bluff body aerodynamics. *J. Wind Engrg. Indust. Aerodyn.* 49, 79–100.
- Vickery, B.J., 1966. Fluctuating lift and drag on a long cylinder of square cross-section in a smooth and in a turbulent stream. *J. Fluid Mech.* 25, 481–494.